Atmos. Chem. Phys. Discuss., 14, 5495–5533, 2014
www.atmos-chem-phys-discuss.net/14/5495/2014/
doi:10.5194/acpd-14-5495-2014


Atmospheric Chemistry and Physics
Open Access
Discussions



# African dust outbreaks over the western Mediterranean basin: 11 year characterization of atmospheric circulation patterns and dust source areas

**P. Salvador[1], S. Alonso[2,3], J. Pey[2,4], B. Artíñano[1], J. J. de Bustos[3], A. Alastuey[2], and X. Querol[2]**

[1]Environmental Department of the Research Center for Energy, Environment and Technology (CIEMAT) – Unidad Asociada en Contaminación Atmosférica CSIC-CIEMAT, Avenida Complutense 40, 28040 Madrid, Spain
[2]Institute of Environmental Assessment & Water Research (IDÆA-CSIC). c/Jordi Girona 18, 08034 Barcelona, Spain
[3]Centro de Investigación Atmosférica de Izaña, Agencia Estatal de Meteorología (AEMET) c/La Marina 20, Santa Cruz de Tenerife 38071, Spain
[4]{Aix-Marseille Université CNRS, LCE FRE 3416, Marseille, 13331, France

Received: 13 January 2014 – Accepted: 11 February 2014 – Published: 3 March 2014

Correspondence to: P. Salvador (pedro.salvador@ciemat.es)

Published by Copernicus Publications on behalf of the European Geosciences Union.

## Abstract

The occurrence of African dust outbreaks over the western Mediterranean basin were identified on an 11 year period (2001–2011). $PM_{10}$ daily data from nine regional background air quality monitoring sites across the study area were compiled and the net dust load transported during each event was estimated. Then, the main atmospheric circulation patterns causing the transport of African air masses, were characterized by mean of an objective classification methodology of atmospheric variables fields. Next, the potential source areas of mineral dust, associated to each circulation pattern were identified by trajectory statistical methods. Finally, an impact index was calculated to estimate the incidence of the African dust outbreaks produced during each circulation pattern, on the levels of dust load in $PM_{10}$ concentrations recorded in the different regions. Our results indicate that the values of the impact index and the areas affected by African dust, strongly depended on the atmospheric circulation pattern. Four circulation types were obtained by the classification procedure. Two of them (CT-1 and CT-4) occurred predominantly during the warm season, bringing dust from areas of Algeria, Tunisia, Western Sahara, western Libya and Mauritania. African dust outbreaks produced during the CT-4 were the most frequent across the period of study, generating the highest impact index over southern, central and eastern regions of the Iberian Peninsula as well as over the Balearic Islands. Conversely, the events caused by the CT-1 encompassed the highest impact index over the western areas of the Iberian Peninsula. The two remaining circulation types (CT-2 and CT-3) were more frequently observed during the spring season. The prevailing flows generated by these two atmospheric circulation patterns, carried mineral dust from areas of Algeria, Tunisia and Western Sahara, giving rise to higher values of the impact index from eastern to western areas of the western Mediterranean basin.





ACPD
14, 5495–5533, 2014

## 1 Introduction

Atmospheric circulation can be described by circulation patterns. A circulation pattern means a field of sea level pressure, geopotential height, or another variable describing atmospheric circulation that is defined for each time instant of the analysis (e.g., hour, day, month) and usually on a regular grid (Huth et al., 2008). At present, various classification methods of circulation patterns are used in many fields of the atmospheric sciences, from weather prediction to synoptic and statistical climatology.

It is well known that significant amounts of African dust are transported westward, towards the Caribbean, the eastern coasts of North America and South America (Prospero et al., 1981; Prospero, 1999; Prospero and Lamb, 2003). Large quantities of mineral dust are also carried across the Mediterranean basin to Europe and the Middle East (Moulin et al., 1998). During such African Dust Outbreaks (ADO) mineral dust represents a significant contribution to daily $PM_{10}$ levels registered at rural and urban monitoring sites in the Mediterranean Basin (Querol et al., 1998, 2004; 2008, 2009; Escudero et al., 2007a; Gerasopoulos et al., 2006; Bouchlaghem et al., 2009; Pey et al., 2013). Some recent studies demonstrated that a relevant percentage of the exceedances of the $PM_{10}$ daily limit value ($50\,\mu g\,m^{-3}$ after the 2008/50/EC European Directive) registered at these sites, can be exclusively attributed to the net African dust load (ADL) transported during ADO (Escudero et al., 2007b; Viana et al., 2010; Salvador et al., 2013).

Previous studies have explained the important differences between the seasonal occurrence of ADO and the impact of the ADL on ambient concentrations of particulate matter over the western, central and eastern Mediterranean basin (Moulin et al., 1998; Querol et al., 2009; Pey et al., 2013). In this study we will focus on the atmospheric processes which originate the transport of African dust towards the western Mediterranean basin.

With the aim to document the occurrence of ADO over different areas of the western Mediterranean basin and to characterize their seasonal trends, air mass classifications





ACPD
14, 5495–5533, 2014

were frequently carried out by means of backward air trajectories, either by straightforward attribution of their origin (Querol et al., 1998, 2004; Artíñano et al., 2001; Rodríguez et al., 2001) or cluster analysis (Salvador et al., 2008, 2013). Otherwise, different interpretations of the meteorological scenarios causing ADO were performed. Many studies have shown specific days of the study period as examples of the most outstanding synoptic situations favoring the transport of African air masses (Rodríguez et al., 2001; Viana et al., 2003; Querol et al., 2009). Escudero et al. (2005) generated composite maps of sea level pressure and geopotential height at 850 and 700 hPa levels, by averaging the first day of each ADO over eastern Spain during 1996–2002, after a visual classification of events. Salvador et al. (2013) grouped air masses arriving on a daily basis over the centre of the Iberian Peninsula during 2001–2008, into homogeneous groups by means of a cluster analysis of back trajectories. Trajectories coming from North-African regions were grouped into a single cluster. They were used to create seasonally composite 850 hPa geopotential height maps.

The results obtained in these works could be considered as approaches on the characterization of ADO over specific areas of the western Mediterranean basin from a meteorological perspective. With the aim of yielding a more systematic perspective, this study deals with this region as a whole. All the ADO occurring in this area from 2001 to 2011 were analyzed. Additionally, an estimation of the ADL contributing to the $PM_{10}$ daily mean levels during each event, was obtained for each region of study. Such a long temporal series of ADO occurrence and ADL estimates in $PM_{10}$ is hardly found in the literature. On the basis of this data set, among others, the occurrence of ADO across the whole Mediterranean basin was analyzed by Pey et al. (2013). Issues related to dust concentrations, seasonal patterns and frequency of the events across the Mediterranean were discussed and evaluated. In this study the main atmospheric processes which give rise to the ADO are characterized and the source areas of dust are identified using different objective statistical procedures. The seasonality and the geographical differences within the areas of study, of the occurrence of the ADO are described.





ACPD
14, 5495–5533, 2014

Firstly, daily patterns of geopotential height at the 850 hPa topography corresponding to episodic days were grouped into homogeneous groups by non-hierarchical *k*-means cluster analysis, each one representing a characteristic atmospheric circulation type. Synoptic situations which give rise to these circulation types, were characterized by composite synoptic maps of sea level pressure and geopotential height at the 850 and 700 hPa topographies. The seasonal occurrence of ADO during each circulation type, was analyzed. Then, the potential source areas of the mineral dust transported during the different circulation types were estimated by trajectory statistical methods. Finally an estimation of the effects of the ADO on the ambient air levels of $PM_{10}$ recorded in the different regions was carried out by means of an impact index.

## 2 Methodology

During the 2001–2011 period, the occurrence of ADO over different regions of the western Mediterranean basin was identified using a robust methodology, which consists in the daily interpretation of meteorological products and air masses back-trajectories. The procedure can be found elsewhere (Escudero et al., 2005, 2007b) and consequently will not be described here in detail.

Then, daily data from nine regional background air quality monitoring sites were obtained during this 11 year period, to evaluate the African dust contributions and to assess their impact on $PM_{10}$ levels. Table 1 lists the various stations used in this study. Seven out of the nine stations are members of EMEP (Co-operative Programme for Monitoring and Evaluation of the Long-Range Transmission of Air Pollutants in Europe). Of the remaining sites, Bellver belongs to the Balearic Islands Regional Air Quality Network whereas Monagrega is part of the ENDESA (Empresa Nacional de Electricidad S.A.) Air Quality Network. 2 different techniques have been used to determine $PM_{10}$ concentrations: gravimetric determinations at the EMEP sites and real time monitors based on Beta gauge attenuation at Monagrega and Bellver. In these two monitoring sites the real time concentrations were corrected against the gravimetric ones. Since





ACPD
14, 5495–5533, 2014

only the official data reported to the European Commission are used in this work, their quality is guaranteed.

These monitoring sites were selected according to data coverage and geographical location criteria. They were the regional background sites with the best data coverage of $PM_{10}$ daily mean values in the period of study ($PM_{10}$ daily data coverage ranging from 84 % to 99 %). Besides, they were distributed throughout the Iberian Peninsula and the Balearic Islands, covering southeastern, southwestern, central, eastern, northeastern, northern and northwestern regions (Fig. 1a). It should be noted that until the year 2004, no rural background station was recording $PM_{10}$ concentration levels on a regular basis in Portugal. For this reason Portugal was not considered in this work.

A procedure for the quantification of the net African dust load transported during each ADO was applied to estimate the impact of the African dust contributions on the $PM_{10}$ daily records. Such methodology is based on the identification of days under the influence of African dust and a statistical analysis based on the calculation of the 30 days moving 40th percentile for the different regional background $PM_{10}$ time series (not containing the $PM_{10}$ values when African dust was detected). This percentile is an indicator of the non-African regional background to be subtracted from the daily $PM_{10}$ levels during African dust outbreaks and thus allows calculating the daily values of ADL. The feasibility of this method was demonstrated by different approaches in Escudero et al. (2007b) and Viana et al. (2010).

This methodology became the Spanish and Portuguese reference method to identify and quantify African dust contributions to $PM_{10}$ levels since 2004. The method is also applicable across the whole Southern Europe, as demonstrated by Querol et al. (2009) and more recently by Pey et al. (2013). Currently, this is one of the official methods recommended by the European Commission for evaluating the occurrence of ADO and quantifying its contributions (Commission staff working paper, 2011).

As a consequence of this preliminary analysis, days contributing with a positive value of ADL in at least, one of the 9 regional background monitoring sites during the 2001–





ACPD
14, 5495–5533, 2014

2011 period, were identified. Henceforth they will be referred to as "episodic days". This study will focus on such episodic days.

### 2.1 Circulation classifications methodology

The main principle of classifying a sample of objects is to generate clusters in the multidimensional space spanned by the parameters, each comprising objects of highest similarity. Non-hierarchical methods choose a specified number of clusters, $k$, and then loops through all the objects in the data set. In the first step of the $k$-means cluster analysis procedure, $k$ seed partitions are created as first guesses and then used for further optimization. In this work a selection of conditions defining different daily circulation types were carried out. Such classifications are known as "circulation classifications" (Huth et al., 2008). During the loop through the objects, each object is assigned to a cluster depending on one of many measures of similarity or dissimilarity that may be chosen for the procedure. The Euclidean distance ($D$) between the objects and its cluster centroids (the seed partitions in the first iteration and the average of all the members of the cluster in the next ones) was used in this study:

$$D\left(X_i,\overline{X}_j\right) = \left[\sum_{l=1}^{m}\left(X_{il}-\overline{X}_{jl}\right)^2\right]^{1/2}. \tag{1}$$

Where $m$ is the number of parameters (grid points in this case) describing the objects, $i$ is the object number and $\overline{X}$ is the centroid of each cluster.

Starting from such a seed partition the objects were checked sequentially and were reassigned from one cluster to another, if that reduces within cluster variance (WCV):

$$\text{WCV} = \sum_{j=1}^{k}\sum_{i\in C_j} D\left(X_i,\overline{X}_j\right)^2. \tag{2}$$

This parameter measures the degree of dissimilarity within the resulting clusters of a certain partition. After each reassignment the cluster centroids have to be updated





ACPD
14, 5495–5533, 2014

for subsequent tests on reassignments. The iterative optimization process ends if no further reassignment can increase the explained cluster variance, that is, convergence to a local optimum has been reached.

One advantage of the non-hierarchical methods is that they allow objects to change cluster membership during each loop over the data set, so that an assignment to a cluster is not permanent throughout the procedure. Some authors (Gong and Richman, 1995; Michelangeli et al., 1995; Philipp et al., 2007) showed that nonhierarchical k-means outperforms hierarchical cluster analysis in general. However, several subjective decisions must be taken across the procedure, e.g. the choice of the dissimilarity measure and the number of classes.

The appropriate number of clusters was determined by computing the percentage change in WCV, as a function of the number of the clusters.

$$\%\Delta \mathrm{WCV}_n = \left(\mathrm{WCV}_n - \mathrm{WCV}_{n-1}\right)/\mathrm{WCV}_n. \quad (3)$$

It represents the percent change of the measure of variance at number of clusters $n$. This statistic increases abruptly as clusters which are significantly different are joined, helping to choose the best number of clusters to be retained (Dorling et al., 1992).

In this study daily fields of sea level pressure and geopotential height at the 850 and 700 hpa levels, were obtained from the ERA-Interim Archive at ECMWF (European Centre for Medium-Range Weather Forecasts) for the period 2001–2011. The ERA-Interim atmospheric model and reanalysis system uses cycle 31r2 of ECMWF's Integrated Forecast System, which was configured for the following spatial resolution: 60 levels in the vertical, with the top level at 0.1 hPa; T255 spherical-harmonic representation for the basic dynamical fields; a reduced Gaussian grid with approximately uniform 79 km spacing for surface and other grid-point fields. Additional information is contained in Dee et al. (2011). Next, a nonhierarchical k-means cluster analysis method was applied for classifying time series of daily fields of geopotential height at the 850 hPa topography, into similar groups or "circulation types" (Huth et al., 2008).





ACPD
14, 5495–5533, 2014

It should be noted that, unlike weather type classification, circulation pattern classification is based on just one parameter of atmospheric circulation and its classification into leading circulation patterns is completely independent from meteorological surface conditions (Yarnal, 1993). As explained by Huth et al. (2008) the majority of circulation classifications use SLP and/or geopotential heights in lower to middle troposphere (up to 500 hPa) defined on a regular latitude-longitude grid. Usually one level is used as an input. Studies using multiple levels (Kidson, 1997; Romero et al., 1999) indicate that owing to a high degree of dependence among individual layers, the inclusion of additional levels yields only little extra information over using a single level. Daily fields of geopotential height at the 850 hPa topography were selected, because in most of the cases they correctly describe the mean transport wind at a synoptic scale during ADO towards the western Mediterranean basin (Moulin et al., 1998; Querol et al., 1998; Salvador et al., 2004). In fact, previous studies stated that the transport of African dust towards this area mostly occurs at relatively high atmospheric levels (Escudero et al., 2005; Querol et al., 2009; Pey et al., 2013). The Atlas Mountains range, extending from Western Sahara towards Tunisia, hinders the transport of dust at low altitudes from occurring.

### 2.2 Identification of potential source areas of dust

It is recognized that the statistical analysis of a great number of back trajectories from receptor sites has turned out to be a valuable tool to identify sources and sinks of atmospheric trace substances or to reconstruct their average spatial distribution (Scheifinger and Kaiser, 2007). Trajectory statistical methods are effective and computationally fast procedures which allow simultaneous computational treatment of air mass back-trajectories and of PM concentrations at one or several receptor points. In spite of the fact that the effect of dispersion and removal during transport are not considered by single trajectories, these methods delivers first hints on potential source areas if applied within the frame of the mean residence time of the considered substance (Stohl et al., 1998).





ACPD
14, 5495–5533, 2014

In this study the Redistributed Concentration Field (RCF) method was used to identify potential source areas of the mineral dust transported during ADO towards Spanish regions. This technique consists of assigning concentration values of ADL measured at the receptor sites to corresponding air parcel backward trajectories. A logarithmic mean concentration is calculated for each grid cell of the spatial domain, by using as a weighting factor the time spent by the air parcel over the cell. A confidence interval for the mean concentration of each cell is calculated and the concentration field is smoothed with a 9-point filter imposing the restriction that the values must be kept within their confidence interval. The smoothing is repeated until the change in the concentration field is less than a prespecified value. Finally, this preliminary CF is used for an iterative redistribution of the concentrations along the trajectories, to obtain the final RCF. Specific details on the computation of CF and RCF can be found elsewhere (Seibert et al., 1994; Stohl, 1996). Numerous studies have found that RCF are able to accurately determine pollutant source locations, transport pathways or even to reproduce their emission inventories (Stohl, 1996; Wotawa and and Kröger, 1999; Lupu and Maenhaut, 2002; Han et al., 2004; Salvador et al., 2007, 2010).

5 day backward 3-D air trajectories arriving at all of the 9 sampling sites at 00:00, 06:00, 12:00 and 18:00 UTC were computed for each day of the 2001–2011 period, using the HYSPLIT model (Draxler and Rolph, 2003). Fixed height of 1500 m a.s.l. was chosen as the air masses arrival height, because this altitude approximately coincides with the 850 hPa geopotential height topography. In all, more than 22 000 trajectories corresponding to episodic days were available for analysis, each with 120 endpoints.

A RCF was thus computed for each circulation type, over the region defined by 12–60° N and 28° W–24° E. For each 2° longitude × 2° latitude grid cell, a weighted concentration of ADL was computed using the procedure defined by Stohl (1996). Zeng and Hopke (1989) were the first authors to propose pooling data sets from different sampling sites with the aim of increasing the number of trajectory endpoints within grid cells and hence to approach their true locations as the random errors will be averaged away. Lupu and Maenhaut (2002) demonstrated that calculating RCF with data from several



Discussion Paper | Discussion Paper | Discussion Paper | Discussion Paper |

ACPD
14, 5495–5533, 2014

African dust outbreaks over the western Mediterranean basin

P. Salvador et al.

locations improved their spatial resolution. For this reason the ADL values registered during episodic days at all the sampling sites, were used to compute each RCF.

### 2.3 Estimation of the impact index

With the aim to evaluate the impact of each circulation type on the levels of ADL registered at the regional background stations during ADO, an impact index (II) was defined. This parameter combined the frequency of occurrence of each circulation pattern with the mean ADL levels recorded during each of them at any sampling site.

$$\mathrm{II}_i = (\mathrm{ADL}_i \cdot N_i)/(\mathrm{ADL} \cdot N_t) \cdot 100. \tag{4}$$

Where, $\mathrm{II}_i$ is the impact index for any site associated to the synoptic situation $i$, $\mathrm{ADL}_i$ is the average value of ADL registered at this site during episodic days grouped into the synoptic situation $i$, $N_i$ is the number of episodic days in this site grouped into the synoptic situation $i$, ADL is the average value of ADL for all the episodic days produced in the site and Nt is the total number of episodic days in this site. For any site:

$$\sum_{i=1}^{4} \mathrm{II}_i = 100\,\%. \tag{5}$$

## 3 Results and discussion

### 3.1 Circulation classifications

During the period 2001–2011, 1592 episodic days were identified (on average 145 episodic days per year) increasing the daily concentration levels of $PM_{10}$ recorded in regional background air quality monitoring stations, due to African mineral dust (Table 2). The highest number of episodic days was recorded in 2007 (187 days) and the lowest in 2005 (125 days).





ACPD
14, 5495–5533, 2014

The occurrence of episodic days showed an increasing gradient from the N (21 % at O Saviñao and Niembro) to the S (65 % at Viznar) (Fig. 1b). At most southern locations it is evident a higher frequency of episodic days, due to the higher proximity to the African mainland.

26 % of the episodic days (409 days) were detected only at one of the sampling sites. Some of these episodic days corresponded to ADO with short duration, which only transported dust to one of the regions. Otherwise during ADO with duration of several days, mineral dust could be transported to further areas, being firstly detected at borderline sites such as Barcarrota (18 % of the episodic days detected only in this site), Viznar (22 %) and Bellver (46 %). Otherwise, 3 % of the episodic days (41 days) were registered simultaneously in all of the stations, during the most intense ADO.

On average the highest number of episodic days was recorded, in summer (June–August) followed by those registered in the spring (March–May) and the autumn (September–November) months. The lowest number of episodic days was recorded from December to February (Table 2).

The application of the methodology exposed in Sect. 2.1, to find an appropriate number of clusters in a given dataset, showed that for the period 2001–2011 ADO were preferentially generated by 4 circulation types.

Figure 2 shows the 4 final cluster centroids of the geopotential height at the 850 hPa level, after the last iteration in the clustering procedure. Composite synoptic maps calculated by averaging the sea level pressure and the geopotential height at the 700 hPa level, using the data corresponding to all episodic days assigned to a particular cluster, are depicted in Figs. S1 and S2 (Supplement). From now on, the four circulation types resulting from the circulation classification will be referred to as CT-1, CT-2, CT-3 and CT-4.

CT-1 centroid illustrated a synoptic meteorological scenario, characterized by a relative low pressure system observed at the 850 and 700 hPa levels west or southwest of the Iberian Peninsula coast and by an upper level high, located over northern Algeria (Fig. 2a). The so called North African high is a common synoptic feature in all the circulation types giving rise to ADO over the western Mediterranean basin. It is produced by the intense heating of the North African surface which generates the development of thermal lows. As a consequence, a compensatory high pressure system is formed at higher altitudes over different geographical locations, depending on the circulation pattern. CT-1 favored the advection of African air masses towards the Iberian Peninsula by south and southwestern winds in the upper atmospheric levels.

The CT-2 composite 850 hPa geopotential height field was characterized by a shift of the North African high to the west and a trough placed over the western Iberian Peninsula coast. A small low pressure system, centered over Morocco, was also noticeable (Fig. 2b). This synoptic meteorological situation generated southwestern winds over the Iberian Peninsula. The composite 700 hPa geopotential height field illustrated a clear south-westerly wind flow with a strong high in the southern Algeria, carrying warm air onto the western Mediterranean basin (Fig. S2b).

It should be noted that other authors identified meteorological scenarios dominated by Atlantic depressions between January and June, inducing transport of African dust towards southern and eastern Spain (Rodríguez et al., 2002; Escudero et al., 2005). Clusters 1 and 2 gathered these scenarios, discriminating between those in which the North African was located over northeastern Algeria and Tunisia (CT-1) or at more eastern locations (CT-2).

The CT-3 centroid showed a strong high pressure system extended over eastern Argelia and Libya in the map of geopotential height at the 850 hPa level. Besides, a strong longitudinal baric gradient produced by a strong Icelandic low and weak Azores high, which is displaced towards the southwest, caused a clear zonal circulation over the Iberian Peninsula (Fig. 2c). This circulation type was not associated in previous studies with dust transport over the western Mediterranean basin.

The most remarkable feature of the synoptic situation described by the CT-4 centroid, was the development of an intense North African high over northeastern Algeria and Tunisia, advecting warm African air masses onto the Iberian Peninsula from southern and southeastern areas (Fig. 2d). At 700 hPa, the North African high was extended over Western Sahara, Mali and Mauritania, inducing the transport of air masses from these areas towards the Iberian Peninsula and the western Mediterranean basin. At sea level, an extension of the Azores high over central Europe and a weak pressure gradient, inhibited the transport of air masses at low altitudes. This was the most frequent synoptic meteorological situation causing ADO over eastern (Rodríguez et al., 2002; Escudero et al., 2005) and central (Salvador et al., 2013) Spain.

The most frequent circulation types were CT-4 and CT-2, representing 33 % and 31 % of the episodic days, respectively. CT-1 accounted for 24 % of the episodic days whereas CT-3 grouped the transport regimes less frequently observed. It represented only 12 % of the episodic days. Figure 3 shows the monthly distribution of occurrence of the circulation types during the period of study. The number and seasonal frequency of episodic days during each year of the period 2001–2011 by circulation type can be consulted in Tables S1 and S2, respectively (Supplement).

Trend estimates of the occurrence of ADO were undertaken, using the OpenAir data analysis tools (Carslaw and Ropkins, 2012). The magnitude of the trend was expressed as a slope using the Theil-Sen method (Hirsch et al., 1982). Smooth trends in the monthly mean concentrations of pollutants were also determined using Generalized Additive Modelling (Carslaw et al., 2007) and represented in Fig. 3. The monthly number of episodic days produced during the different circulation types, did not show a significant trend (neither upward nor downward). These results indicate that the occurrence of ADO over the Iberian Peninsula and the Balearic Islands under the four prevalent circulation types obtained, maintained a steady tendency during the period 2001–2011. This fact is evidenced in Fig. 3 by the horizontal lines, representing the smooth trends.

Table 2 and Fig. 3 illustrate that a marked seasonal pattern is observed in the occurrence of the different circulation types. There was a clear seasonal trend towards a higher frequency of CT-1 episodic days during the summer months and in lesser extent during spring and autumn. The episodic days occurred during CT-2, were more frequent during the spring and the summer months. The meteorological scenarios rep-





ACPD
14, 5495–5533, 2014

resented by the CT-3, occurred predominantly in spring and autumn and less frequently during summer. In opposition, CT-4 episodic days were more likely registered in summer.

Moulin et al. (1997) found that interannual variations in dust transport from North Africa towards the Atlantic Ocean and the Mediterranean Sea, were well correlated with the climatic variability defined by the North Atlantic Oscillation (NAO) index. This index was defined by Hurrell (1995), and accounts for the difference between the normalized sea-level atmospheric pressures between Lisbon, Portugal and Stykkisholmur, Iceland. It has the limitation that these stations are fixed in space and thus may not track the movement of the NAO centers of action through the annual cycle. Besides, individual station pressure readings can be noisy due to small-scale and transient meteorological phenomena unrelated to the NAO.

When this pressure gradient between the Icelandic low and the subtropical high is more intense than normal (positive NAO) the westerly winds are stronger across northern Europe. This brings Atlantic air masses over the continent, associated with mild temperatures and higher precipitation and dryer conditions across southern Europe. When the pressure gradient is less intense than normal (negative NAO) the track of westerly Atlantic winds is observed at lower latitudes, bringing stronger than normal winds over the Mediterranean. Moreover, in recent published works, winter (Cusack et al., 2012) and summer (Pey et al., 2013) periods with positive and negative NAO index were associated with more and less frequent ADO, respectively, over areas of the Iberian Peninsula and the north-western region of the Mediterranean Basin.

In this work annual and monthly mean NAO index for the 2001–2011 period were obtained from the NOAA data center (http://www.cpc.ncep.noaa.gov/products/precip/CWlink/pna/nao.shtml) and compared with the occurrence of episodic days according to the four circulation types. They did not always show a statistically significant linear correlation across all the seasons and the years of the period 2001–2011. This fact evidences that other factors related with large-scale dynamical features apart from





ACPD
14, 5495–5533, 2014

NAO index, contributes to the year-to-year variability of the occurrence of ADO and the intensity of dust export (Moulin et al., 1997).

Anyway, a remarkable result was found in relation with the development of different circulation types during periods with a high or low NAO index. Figure 4a depicts the good fitting between the annual occurrence of CT-2 and CT-3 episodic days and the corresponding annual NAO index values. This behaviour was especially intense during spring (Fig. 4b). In this period, CT-2 as well as CT-1, showed a positive linear relationship with the value of the NAO index. The opposite was found with the CT-3. It should be noted that the year 2010 was excluded from the correlation plot (Fig. 4a) owing to the atypical low values of the NAO index obtained across all the seasons (annual NAO index = −1.65). It is evident that this year was governed by anomalous atmospheric patterns.

This fact suggests that during specific low-NAO periods, the transport of African dust towards the western Mediterranean basin could be achieved, in spite of the fact that zonal flows prevailed over this area. This situation was depicted in Fig. 5a, which represents the mean geopotential height at 850 hPa during episodic days in spring 2005. This was the year with the lower NAO index value in spring. The advection of Atlantic air masses was produced at lower latitudes than usual (grey arrow) but the presence of the high pressure system extended over eastern Algeria, Tunisia and Libya, allowed the transport of the African air masses (white arrow) towards the eastern side of the Iberian Peninsula and the Balearic Islands. The similarity between Figs. 5a and 2c, illustrates the prevalence of the CT-3 in this period.

On the contrary, periods with higher than normal NAO index values, revealed a different synoptic meteorological situation. During spring 2011 (Fig. 5b) the advection of Atlantic air masses took place at latitudes higher than 45° N, whereas the low pressure system located over 35° N–15° W and the high pressure system extended again over eastern Algeria, Tunisia and Libya, favored African air masses moving northward. In this period 50 episodic days were identified, most of them caused by CT-1 (24 %) and CT-2 (52 %).





ACPD
14, 5495–5533, 2014

### 3.2 Identification of source areas of dust

RCF results were reported on geographical maps as a result of the interpolation of the weighted concentrations in the grid cells. They showed concentration gradients across potential sources. It is important to note that these maps do not provide an emission inventory of a pollutant but rather show those source areas whose emissions can be transported to the measurement site by prevailing synoptic winds (Vinogradova, 2000).

To assess quantitatively the weighted concentrations, they were distributed in equal intervals from the lowest to the highest values. Thus, cells with weighted concentrations in the higher and lower value ranges indicated that, on average, air parcels residing over these cells resulted in high and low concentrations, respectively, of the ADL at the receptor sites. RCF maps obtained for ADL in $PM_{10}$ for the different circulation types are showed in Fig. 6. RCF maps obtained during the seasons with a higher frequency of occurrence for each circulation type are represented in Fig. S3 as Supplement.

Prospero et al. (2002) have shown that dust sources are usually associated with topographical lows in arid regions where runoff and flooding have created lacustrine and alluvial sediments. These sediments are composed of fine particles which are easily eroded by winds. Ginoux et al. (2001) determined the global distribution of dust sources taking into account this so called “topographic hypothesis” and creating a source function $S$, which represents the probability to have accumulated transportable sediments at land surface with bare soil. African dust sources estimated this way are consistent with studies that used satellite products to locate major dust sources such as TOMS absorbing aerosol index (Prospero et al., 2002) or MODIS Deep Blue aerosol products (Ginoux et al., 2010, 2012). The values of the source function $S$ are represented in $0.25^\circ \times 0.25^\circ$ grid cells in Fig. 7.

Most of the prominent sources identified in the RCF maps (Fig. 6) as the greatest potential sources of mineral dust, agreed fairly well with maxima in the dust source function map (Fig. 7). The intense dust emission area located over Algeria centered at 26° N–0° E and extending from 22° S to 30° N, was identified as a potential source area





ACPD
14, 5495–5533, 2014

in the RCF obtained for CT-1, CT-2 and CT-4 episodic days. The Grand Erg Oriental, a large basin (200 000 $km^2$) with sand seas (Prospero et al., 2002) is considered as the main source area of mineral dust in this area.

The series of sources starting near the west coast of North Africa at 23° N–16° W and extending to the north and northeast to 26–27° N and 6–7° W over Western Sahara and northern Mauritania, were identified in the CT-1 and CT-3 RCF. This potential source area included hydrologic sources such as lakes in the Tiris Zemmour region in Northern Mauritania (Ginoux et al., 2012). Source areas are attributed to a hydrological origin based on the presence of ephemeral water bodies such as streams, rivers, lakes, and playas which contain deposits of clay, silt, and salts (Prospero et al., 2002).

Besides, the region located between Tunisia and northeast Algeria, in an area centered at 34° N–8° E, was also distinguished as a source area of dust in the CT-1, CT-2 and CT-3 RCF. This area groups ephemeral lakes such as the Chott Jerid in Tunisia and the Chott Melrhir in northeastern Algeria and the sand seas in the Grand Erg Oriental (Prospero et al., 2002; Ginoux et al., 2012).

All these areas are essentially natural sources (dust emitted from land surfaces where land use is less than 30 %, Ginoux et al., 2012). They are active during all the months of the year, but the maximum activity is currently reached from April to September (Prospero et al., 2002). Other less intense source areas were identified over Mauritania and western Libya.

### 3.3 Influence of the different circulation types on the ADL levels in $PM_{10}$

Table 3 shows the ranges of variation of the II values for all the circulation types and the sampling locations. On average, CT-1 had the largest II values in the most western located stations, Barcarrota and O Saviñao whereas for the other stations the highest II corresponded to the CT-4. This is probably a consequence of the fact that maximum activity of most of the African sources of dust, is currently reached in summer (Prospero et al., 2002).





ACPD
14, 5495–5533, 2014

In order to demonstrate that these II were strongly linked to the geographical location of the sampling sites, interpolation maps of their values were calculated for each circulation type (Fig. 8).

Interpolation map for the CT-1 II values showed an east to west gradient, so that ADO produced during this circulation type had a higher influence on western Spanish regions (Fig. 8a). This fact could be attributed to the action of the Atlantic low pressure system, which characterized the synoptic situation described in Fig. 2a for CT-1. CT-2 generated similar II values for all the Iberian Peninsula regions. Unlike them, the Balearic Islands II was somewhat higher (Fig. 8b) as a consequence of the typical south-westerly wind flows, generated by these synoptic meteorological situations (Fig. 2b). CT-3 II interpolation map clearly depicts a strong west to east gradient (Fig. 8c) by the prevalent southwestern circulation over the Iberian Peninsula associated to this circulation pattern (Fig. 2c). II values were lower than 10 % at the western sites, rising to 17–18 % at the Levante sites (Zarra, Els Torms and Monagrega) and to 20 % at the Balearic Islands site (Bellver). Interpolation map indicated that the CT-4, generated higher II values at southern, eastern and central areas of the Iberian Península than at western and northern regions and the Balearic Islands (Fig. 8d). It should be noted that the II values of ADO generated by this circulation type, were higher than the other circulation types, for most of the sites. In these cases the air masses were heavily loaded with dust and were transported furthest towards the North owing to the intensity of the North African high pressure system and its proximity to the western Mediterranean basin (Fig. 2d).

## 4 Conclusions

In this work different statistical techniques were applied to a set of 11 years (2001–2011) of African Dust Outbreaks (ADO) occurrence over the western Mediterranean basin with the aim to characterize the prevailing atmospheric circulation patterns and dust source areas. Estimations of the values of African Dust Load in $PM_{10}$ (ADL) during



Discussion Paper | Discussion Paper | Discussion Paper | Discussion Paper |

ACPD

14, 5495–5533, 2014

African dust outbreaks over the western Mediterranean basin

P. Salvador et al.

each event were obtained at 9 regional background sites across the western Mediterranean basin and analyzed together with daily fields of meteorological variables and with daily air mass back-trajectories arriving at these sites.

The summer months dominated ADO occurrence (40 % of the total number of episodic days produced during the 2001–2011 period), under two prevailing circulation types (CT-1 and CT-4). Their transport mechanisms were composed of two stages. In the first stage, convective injection of dust from areas of Algeria, Tunisia, Western Sahara, western Libya and Mauritania was produced by the intense surface heating. In the second stage, transport towards the Iberian Peninsula and the Balearic Islands was produced at the upper levels, being driven by the North African high, alone in the case of CT-4 or in combination with a relative low pressure system placed west of the Iberian Peninsula coast in the case of CT-1. ADO produced during the first type of situation (CT-4) were the most frequent across the period of study (33 %), generating the highest II values at southern, eastern and central areas of the Iberian Peninsula and the Balearic Islands. Events generated by the second type of situation (CT-1 – 24 % of the total) produced the highest II at the western areas of the Iberian Peninsula. They were also detected, with a less frequency, in the spring and the autumn months.

The remaining two circulation types (CT-2 and CT-3), were more typically produced during the spring season but also in the summer (CT-2) and the autumn (CT-3) months. Impact index values were in general lower in most regions during CT-2 and mainly during CT-3 when compared to those observed during CT-1 and CT-4. CT-2 accounted for 31 % of the total number of episodic days, whereas CT-3 was the less frequent situation (12 %). They were characterized by a displacement of the North African high to the west and by a stronger baric gradient than the one obtained in the CT-1 and CT-4. South to southwestern winds were the prevailing flows generated by these synoptic situations, transporting mineral dust from areas of Algeria, Tunisia and Western Sahara. Our results indicated a progressive higher influence of the ADO originated during these circulation types towards the west, more evident in the case of the CT-3 than the CT-2. As a consequence, the highest impact index values were obtained in the Balearic

Islands in both cases. The occurrence of the different circulation types was associated with the values of the North Atlantic Oscillation (NAO) index during spring. In fact, this index was observed to influence the frequency of CT-1, CT-2 and CT-3 episodic days across the western Mediterranean basin during spring. In this period higher (lower) than normal values of the NAO index, were associated with higher (lower) frequency of CT-1 and CT-2 episodic days. This suggests that when NAO was more intensely positive, the probability of generating atmospheric circulation types, such as CT-1 and CT-2, leading air masses from North Africa to reach the NW Mediterranean was higher. On the contrary during negative NAO phases in this period, the advection of Atlantic air masses was produced at lower latitudes than usual, thus hindering subtropical air masses to reach the Iberian Peninsula. However during specific events characterized by the presence of the high pressure systems located over eastern Algeria, Tunisia and Libya as in CT-3, the transport of the African air masses towards the eastern side of the Iberian Peninsula and the Balearic Islands could be produced.

The results obtained in this study demonstrate that ADO across the western Mediterranean basin were caused by different atmospheric circulation patterns, which condition their intensity and the areas affected by mineral dust. The four main synoptic meteorological situations that generate this type of events were described in this work and the highest potential source areas of mineral dust, associated to each of them, were also characterized. This information can be used as a complementary tool for their prediction and analysis of aerosol properties as well as their effects on human health, ecosystems or rain composition, distinguishing between air masses coming from different areas of the African continent.

**Supplementary material related to this article is available online at http://www.atmos-chem-phys-discuss.net/14/5495/2014/acpd-14-5495-2014-supplement.zip.**





ACPD
14, 5495–5533, 2014

*Acknowledgements.* This work was funded by the Spanish Ministry of the Environment and Rural and Marine Affairs under the project "Estudio y evaluacion de la contaminacion atmosferica por material particulado y metales en España" (UCA 2009020083) and by research projects GRACCIE-CSD2007-00067, MICROSOL (CGL2011-27020) and VAMOS (CGL2010-19464/CLI). The authors wish to thank the EMEP programme, supplying $PM_{10}$ data used in this study and the NOAA Air Resources Laboratory (ARL) for the provision of the HYSPLIT trajectory model. We acknowledge the Atmospheric Modelling & Weather Forecasting Group in the University of Athens, the Atmospheric Modelling Laboratory from the Barcelona Supercomputing Centre, the Naval Research Laboratory and the SeaWiFS project (NASA) for the provision of the SKIRON, DREAM, NAAPs aerosol maps, and the satellite imagery, respectively.

## References

Artíñano, B., Querol, X., Salvador, P., Rodríguez, S., Alonso, D. G., and Alastuey, A.: Assessment of airborne particulate levels in Spain in relation to the new EU-Directive, Atmos. Environ., 35, S43–S53, 2001.

Bouchlaghem, K., Nsom, B., Latrache, N., and Haj Kacem, H.: Impact of Saharan dust on $PM_{10}$ concentration in the Mediterranean Tunisian coasts, Atmos. Res., 92, 531–539, 2009.

Carslaw, D. C. and Ropkins, K.: Openair – an R package for air quality data analysis, Environ. Modell. Softw., 27–28, 52–61, 2012.

Carslaw, D. C., Beevers, S. D., and Tate, J. E.: Modelling and assessing trends in traffic-related emissions using a generalised additive modelling approach, Atmos. Environ., 41, 5289–5299, 2007.

Commission staff working paper, establishing guidelines for demonstration and subtraction of exceedances attributable to natural sources under the Directive 2008/50/EC on ambient air quality and cleaner air for Europe, Brussels, 15.02.2011. SEC(2011) 208 final, 37 pp., available at: http://ec.europa.eu/environment/air/quality/legislation/pdf/sec_2011_0208.pdf (last access: 2014), 2011.

Cusack, M., Alastuey, A., Pérez, N., Pey, J., and Querol, X.: Trends of particulate matter ($PM_{2.5}$) and chemical composition at a regional background site in the Western Mediterranean over the last nine years (2002–2010), Atmos. Chem. Phys., 12, 8341–8357, doi:10.5194/acp-12-8341-2012, 2012.

Dee, D. P., Uppala, S. M., Simmons, A. J., Berrisford, P., Poli, P., Kobayashi, S., Andrae, U., Balmaseda, M. A., Balsamo, G., Bauer, P., Bechtold, P., Beljaars, A. C. M., van de Berg, L., Bidlot, J., Bormann, N., Delsol, C., Dragani, R., Fuentes, M., Geer, A. J., Haimberger, L., Healy, S. B., Hersbach, H., H'olm, E. V., Isaksen, L., Kallberg, P., Köhler, M., Matricardi, M., McNally, A. P., Monge-Sanz, B. M., Morcrette, J.-J., Park, B.-K., Peubey, C., de Rosnay, P., Tavolato, C., Thépaut, J.-N., and Vitart, F.: The ERA-Interim reanalysis: configuration and performance of the data assimilation system, Q. J. Roy. Meteor. Soc., 137, 553–597, 2011.

Dorling, S. R., Davies, T. D., and Pierce, C. E.: Cluster analysis: a technique for estimating the synoptic meteorological controls on air and precipitation chemistry – method and applications, Atmos. Environ., 26A, 2575–2581, 1992.

Draxler, R. R. and Rolph, G. D.: HYSPLIT (HYbrid Single-Particle Lagrangian Integrated Trajectory), Silver Spring, MD, Model access via NOAA ARL READY Website, available at: http://www.arl.noaa.gov/ready/hysplit4.html (last access: 2014), 2003.

Escudero, M., Castillo, S., Querol, X., Avila, A., Alarcón, M., Viana, M. M., Alastuey, A., Cuevas, E., and Rodríguez, S.: Wet and dry African dust episodes over eastern Spain, J. Geophys. Res., 110, D18S08, doi:10.1029/2004JD004731, 2005.

Escudero, M., Querol, X., Ávila, A., and Cuevas, E.: Origin of the exceedances of the European daily PM limit value in regional background areas of Spain, Atmos. Environ., 41, 730–744, 2007a.

Escudero, M., Querol, X., Pey, J., Alastuey, A., Pérez, N., Ferreira, F., Alonso, S., Rodríguez, S., and Cuevas, E.: A methodology for the quantification of the net African dust load in air quality monitoring networks, Atmos. Environ., 41, 5516–5524, 2007b.

Gerasopoulos, E., Kouvarakis, G., Babasakalis, P., Vrekoussis, M., Putaud, J. P., and Mihalopoulos, N.: Origin and variability of particulate matter ($PM_{10}$) mass concentrations over the Eastern Mediterranean, Atmos. Environ., 40, 4679–4690, 2006.

Ginoux, P., Chin, M., Tegen, I., Prospero, J., Holben, B., Dubovik, O., and Lin, S. J.: Sources and global distributions of dust aerosols simulated with the GOCART model, J. Geophys. Res., 106, 255–273, 2001.

Ginoux, P., Garbuzov, D., and Hsu, H. C.: Identification of anthropogenic and natural dust sources using Moderate Resolution Imaging Spectroradiometer (MODIS) Deep Blue level 2 data, J. Geophys. Res., 115, D05204, doi:10.1029/2009JD012398, 2010.





ACPD
14, 5495–5533, 2014

Ginoux, P., Prospero, J. M., Gill, T. E., Hsu, H. C., and Zhao, M.: Global-scale attribution of anthropogenic and natural dust sources and their emission rates based on MODIS Deep Blue aerosol products, Rev. Geophys., 50, RG3005, doi:10.1029/2012RG000388, 2012.

Gong, X. and Richman, M. B.: On the application of cluster analysis to growing season precipitation data in North America east of the Rockies, J. Climate, 8, 897–931, 1995.

Han, Y., Holsen, T. M., Hopke, P. K., Cheong, J., Kim, H., and Yi, S.: Identification of source locations for atmospheric dry deposition of heavy metals during yellow-sand events in Seoul, Korea in 1998 using hybrid receptor models, Atmos. Environ., 38, 5353–5361, 2004.

Hirsch, R., Slack, J. R., and Smith, R. A.: Techniques of trend analysis for monthly water quality data, Water Resour. Res., 18, 107–121, 1982.

Hurrell, J. W.: Decadal trend in the North Atlantic Oscillation: regional temperatures and precipitations, Science, 269, 676–679, 1995.

Huth, R., Beck, C., Philipp, A., Demuzere, M., Ustrnul, Z., Cahynová, M., Kyselý, J., and Tveito, O. E.: Classifications of atmospheric circulation patterns: recent advances and applications, Ann. NY Acad. Sci., 1146, 105–152, 2008.

Kidson, J. W.: The utility of surface and upper air data in synoptic climatological specification of surface climatic variables, Int. J. Climatol., 17, 399–413, 1997.

Lupu, A. and Maenhaut, W.: Application and comparison of two statistical trajectory techniques for identification of source regions of atmospheric aerosol species, Atmos. Environ., 36, 5607–5618, 2002.

Michelangeli, P. A., Vautard, R., and Legras, B.: Weather regimes: recurrence and quasi stationary, J. Atmos. Sci., 52, 1237–1256, 1995.

Moulin, D., Lambert, C. E., Dulac, F., and Dayan, U.: Control of atmospheric export of dust from North Africa by the North Atlantic Oscillation, Nature, 387, 691–694, 1997.

Moulin, C., Lambert, C. E., Dayan, U., Masson, V., Ramonet, M., Bousquet, P., Legrand, M., Balkanski, Y. J., Guelle, W., Marticorena, B., Bergametti, G., and Dulac, F.: Satellite climatology of African dust transport in the Mediterranean atmosphere, J. Geophys. Res., 103, 13137–13144, 1998.

Pey, J., Querol, X., Alastuey, A., Forastiere, F., and Stafoggia, M.: African dust outbreaks over the Mediterranean Basin during 2001–2011: $PM_{10}$ concentrations, phenomenology and trends, and its relation with synoptic and mesoscale meteorology, Atmos. Chem. Phys., 13, 1395–1410, doi:10.5194/acp-13-1395-2013, 2013.

Philipp, A., Della-Marta, P. M., Jacobeit, J., Fereday, D. R., Jones, P. D., Moberg, A., and Wanner, H.: Long-term variability of daily North-Atlantic-European pressure patterns since 1850 classified by simulated annealing clustering, J. Climate, 20, 4065–4095, 2007.

Prospero, J. M.: Long-term measurements of the transport of African mineral dust to the southeastern United States: implications for regional air quality, J. Geophys. Res., 104, 15917–15927, 1999.

Prospero, J. M. and Lamb, P. J.: African droughts and dust transport to the Caribbean: climate change implications, Science, 7, 1024–1027, doi:10.1126/science.1089915, 2003.

Prospero, J. M., Glaccum, R. A., and Nees, R. T.: Atmospheric transport of soil dust from Africa to South America, Nature, 289, 570–572, 1981.

Prospero, J. M., Ginoux, P., Torres, O., Nicholson, S. E., and Gill, T. E.: Environmental characterization of global sources of atmospheric soil dust identified with the Nimbus 7 Total Ozone Mapping Spectrometer (TOMS) absorbing aerosol product, Rev. Geophys., 40, 1002, doi:10.1029/2000RG000095, 2002.

Querol, X., Alastuey, A., Puicercus, J. A., Mantilla, E., Miró, J. V., López-Soler, A., Plana, F., and Artíñano, B.: Seasonal evolution of suspended particles around a large coal-fired power station: particles levels and sources, Atmos. Environ., 32, 1963–1978, 1998.

Querol, X., Alastuey, A., Rodriguez, S., Viana, M., Artíñano, B., Salvador, P., Mantilla, E., Garcia, S., Fernandez, R., de la Rosa, J., Sanchez, A., Menendez, M., and Gil, J.: Levels of particulate matter in rural, urban and industrial sites in Spain, Sci. Total Environ., 334–335, 359–376, 2004.

Querol, X., Alastuey, A., Moreno, T., Viana, M. M., Castillo, S., Pey, J., Rodriguez, S., Artíñano, B., Salvador, P., Sánchez, M., Garcia, S., Herce, M. D., Fernandez, R., Moreno, S., Negral, L., Minguillón, M., Monfort, E., Sanz, M., Palomo, R., Pinilla, E., Cuevas, E., de la Rosa, J., and Sanchez, A.: Spatial and temporal variations in airborne particulate matter ($PM_{10}$ and $PM_{2.5}$) across Spain 1999–2005, Atmos. Environ., 42, 3964–3979, 2008.

Querol, X., Pey, J., Pandolfi, M., Alastuey, A., Cusack, M., Pérez, N., Moreno, N., Viana, M., Mihalopoulos, N., Kallos, G., and Kleanthous, S.: African dust contributions to mean ambient $PM_{10}$ mass-levels across the Mediterranean basin, Atmos. Environ., 43, 4266–4277, 2009.

Rodríguez, S., Querol, X., Alastuey, A., Kallos, G., and Kakaliagou, O.: Saharan dust contributions to $PM_{10}$ and TSP levels in Southern and Eastern Spain, Atmos. Environ., 35, 2433–2447, 2001.

Romero, R., Sumner, G., Ramis, C., and Genovs, A.: A classification of the atmospheric circulation patterns producing significant daily rainfall in the Spanish Mediterranean area, Int. J. Climatol., 19, 765–785, 1999.
Salvador, P., Artíñano, B., Alonso, D., Querol, X., and Alastuey, A.: Identification and characterisation of sources of $PM_{10}$ in Madrid (Spain) by statistical methods, Atmos. Environ., 38, 435–447, 2004.
Salvador, P., Artíñano, B., Querol, X., Alastuey, A., and Costoya, M.: Characterisation of local and external contributions of atmospheric particulate matter at a background coastal site, Atmos. Environ., 41, 1–17, 2007.
Salvador, P., Artíñano, B., Querol, X., and Alastuey, A.: A combined analysis of backward trajectories and aerosol chemistry to characterise long-range transport episodes of particulate matter: the Madrid Air Basin, a case study, Sci. Total Environ., 390, 495–506, 2008.
Salvador, P., Artíñano, B., Pio, C., Afonso, J., Legrand, M., Puxbaum, H., and Hammer, S.: Evaluation of aerosol sources at European high altitude background sites with trajectory statistical methods, Atmos. Environ., 44, 2316–2329, 2010.
Salvador, P., Artíñano, B., Molero, M., Viana, M., Pey, J., Alastuey, A., and Querol, X.: African dust contribution to ambient aerosol levels across central Spain: characterization of long-range transport episodes of desert dust, Atmos. Res., 127, 117–129, 2013.
Scheifinger, H. and Kaiser, A.: Validation of trajectory statistical methods, Atmos. Environ., 41, 8846–8856, 2007.
Seibert, P., Kromp-Kolb, H., Baltenspenger, U., Jost, D. T., Schwikowski, M., Kasper, A., and Puxbaum, H.: Trajectory Analysis of Aerosol Measurements at High Alpine Sites. A contribution to subproject ALPTRAC, The Proceedings of EUROTRAC Symposium '94, edited by: Borrell, P. M., Borrell, P., Cvitas, T., and Seiler, W., Academic Publishing, The Hague, 689–693, 1994.
Stohl, A.: Trajectory statistics-a new method to establish source–receptor relationships of air pollutants and its application to the transport of particulate sulfate in Europe, Atmos. Environ., 30, 579–587, 1996.
Stohl, A.: Computation, accuracy and applications of trajectories – a review and bibliography, Atmos. Environ., 32, 947–966, 1998.
Viana, M., Querol, X., Alastuey, A., Gangoiti, G., and Menéndez M.: PM levels in the Basque Country (Northern Spain): analysis of a 5 year data record and interpretation of seasonal variations, Atmos. Environ., 37, 2879–2891, 2003.





ACPD
14, 5495–5533, 2014

Viana, M., Salvador, P., Artíñano, B., Querol, X., Alastuey, A., Pey, J., Latz, A. J., Cabañas, M., Moreno, T., García, S., Herce, M., Diez, P., Romero, D., and Fernández, R.: Assessing the performance of methods to detect and quantify African dust in airborne particulates, Environ. Sci. Technol., 44, 8814–8820, 2010.

Vinogradova, A. A.: Anthropogenic pollutants in the Russian Arctic atmosphere: sources and sinks in spring and summer, Atmos. Environ., 34, 5151–5160, 2000.

Wotawa, G. and Kröger H.: Testing the ability of trajectory statistics to reproduce emission inventories of air pollutants in cases of negligible measurement and transport errors, Atmos. Environ., 33, 3037–3043, 1999.

Yarnal, B.: Synoptic Climatology in Environmental Analysis, Belhaven Press, London, UK, 195 pp., 1993.

Zeng, Y. and Hopke, P.: A study of the sources of acid precipitation in Ontario, Canada, Atmos. Environ., 23, 1499–1509, 1989.





ACPD
14, 5495–5533, 2014

**Table 1.** Location, $PM_{10}$ daily data availability during the 2001–2011 period and measurement methods used in the air quality monitoring sites of this study (EMEP stations in bold).

| Site | Location | Latitude | Longitude | m a.s.l. | % Data | Method |
|---|---|---|---|---|---|---|
| **O Saviñao** | NW IP | 42°38′05″ N | 07°42′17″ W | 506 | 90 % | GRAV |
| **Barcarrota** | SW IP | 38°28′22″ N | 06°55′25″ W | 393 | 90 % | GRAV |
| **Viznar** | SE IP | 37°14′14″ N | 03°32′03″ W | 1230 | 93 % | GRAV |
| **Niembro** | N IP | 43°26′21″ N | 04°51′00″ W | 134 | 87 % | GRAV |
| **Risco Llano** | Central IP | 39°32′49″ N | 04°21′02″ W | 917 | 86 % | GRAV |
| **Zarra** | E IP | 39°04′58″ N | 01°06′04″ W | 885 | 94 % | GRAV |
| **Els Torms** | NE IP | 41°23′38″ N | 00°44′05″ E | 470 | 91 % | GRAV |
| Monagrega | NE IP | 40°56′48″ N | 00°17′27″ W | 570 | 99 % | BETA |
| Bellver | Balearic Islands | 39°33′50″ N | 02°37′22″ E | 117 | 84 % | BETA |

IP: Iberian Peninsula; GRAV: Gravimetric; BETA: Beta Attenuation monitor; a.s.l.: above sea level.





ACPD
14, 5495–5533, 2014

**Table 2.** Occurrence of episodic days during the period 2001–2011 and by circulation type (CT-1 to CT-4).

| | 2001–2011 | CT-1 | CT-2 | CT-3 | CT-4 |
|---|---|---|---|---|---|
| *N* | 1592 | 387 | 489 | 196 | 520 |
| Winter | 11 % | 11 % | 10 % | 22 % | 9 % |
| Spring | 27 % | 22 % | 39 % | 37 % | 15 % |
| Summer | 40 % | 45 % | 35 % | 6 % | 53 % |
| Autumn | 22 % | 21 % | 16 % | 35 % | 22 % |

*N* – Number of episodic days.





ACPD
14, 5495–5533, 2014

African dust outbreaks over the western Mediterranean basin

P. Salvador et al.

**Table 3.** Impact Index (II) calculated for each sampling site during each circulation type leading to African Dust Outbreaks (ADO) over the western Mediterranean basin in the period 2001–2011.

| II | CT-1 | CT-2 | CT-3 | CT-4 |
|---|---|---|---|---|
| O Saviñao | 38 % | 24 % | 3 % | 35 % |
| Barcarrota | 37 % | 23 % | 7 % | 33 % |
| Viznar | 26 % | 24 % | 11 % | 39 % |
| Niembro | 31 % | 25 % | 10 % | 34 % |
| Risco Llano | 27 % | 20 % | 10 % | 43 % |
| Zarra | 23 % | 22 % | 17 % | 39 % |
| Els Torms | 20 % | 24 % | 18 % | 38 % |
| Monagrega | 20 % | 22 % | 18 % | 40 % |
| Bellver | 17 % | 31 % | 20 % | 33 % |





ACPD
14, 5495–5533, 2014

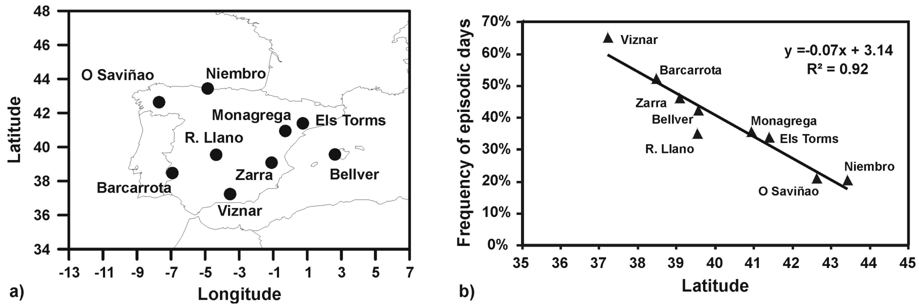


**Fig. 1.** Location of regional background air quality monitoring sites used in this study **(a)** and relationship between their latitudes and the frequency of episodic days registered at them **(b)**.

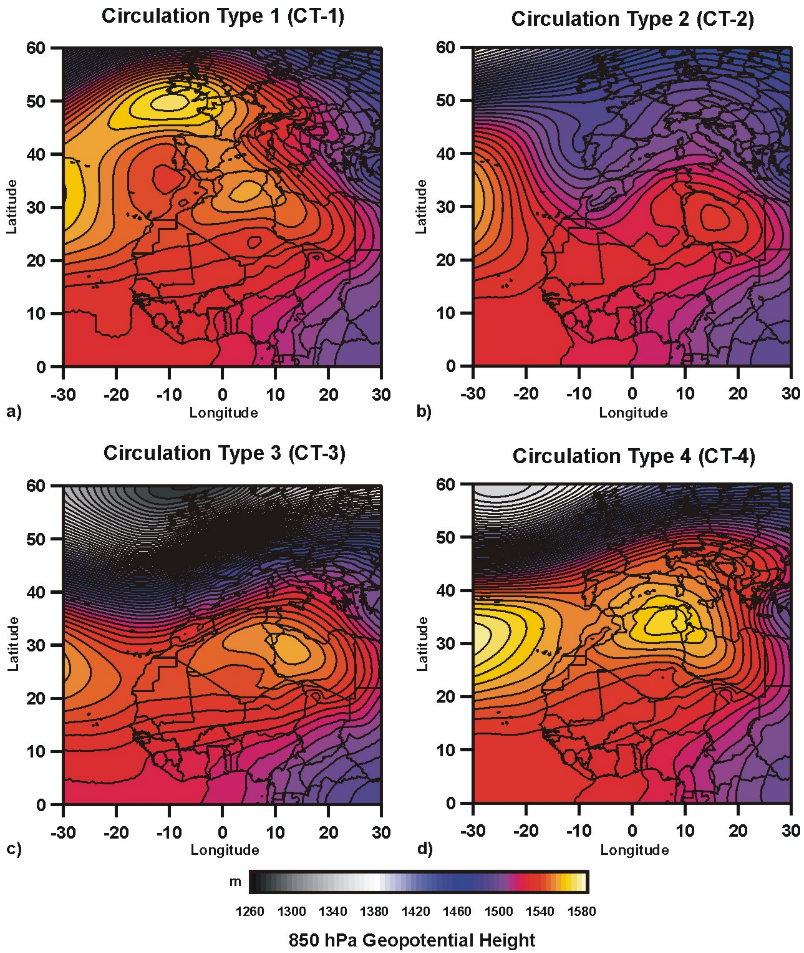


**Fig. 2.** Composite 850 hPa geopotential height (m) representing circulation types leading to ADO over the western Mediterranean basin.

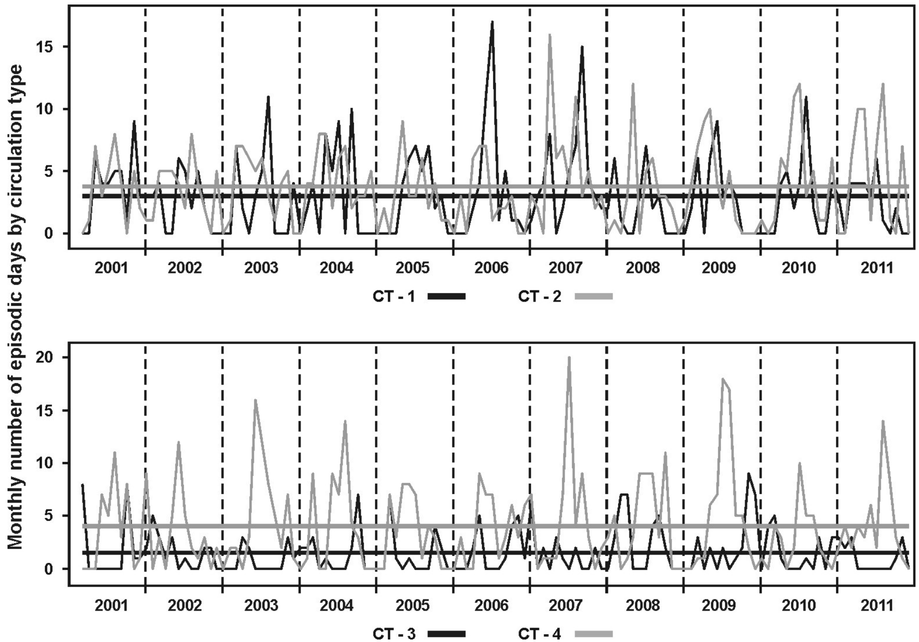


**Fig. 3.** Evolution and smooth trend line in monthly number of episodic days by circulation type (upper: CT-1 and CT-2; bottom: CT-3 and CT-4) registered over the western Mediterranean basin from 2001 to 2011.





ACPD
14, 5495–5533, 2014

African dust outbreaks over the western Mediterranean basin

P. Salvador et al.

Title Page
Abstract | Introduction
Conclusions | References
Tables | Figures
◀| |▶
◀ ▶
Back | Close
Full Screen / Esc
Printer-friendly Version
Interactive Discussion

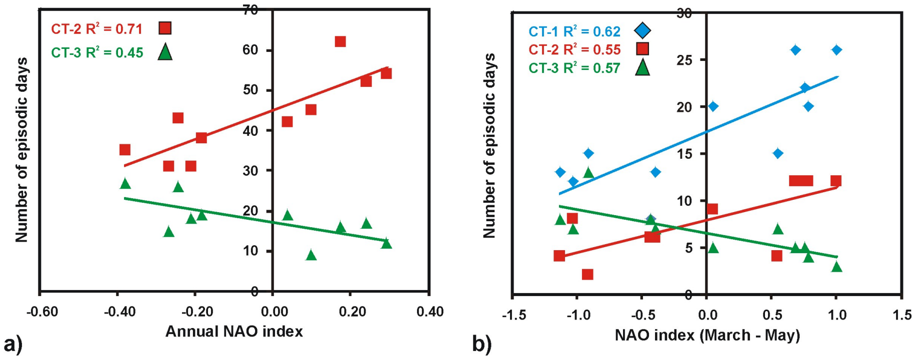


**Fig. 4.** Correlation plot between the annual NAO index **(a)** and the spring (March–May) NAO index **(b)** and the number of episodic days for specific circulation types from 2001 to 2011.





ACPD
14, 5495–5533, 2014

African dust outbreaks over the western Mediterranean basin

P. Salvador et al.

Title Page
Abstract | Introduction
Conclusions | References
Tables | Figures
◀| |▶
◀ ▶
Back | Close
Full Screen / Esc
Printer-friendly Version
Interactive Discussion

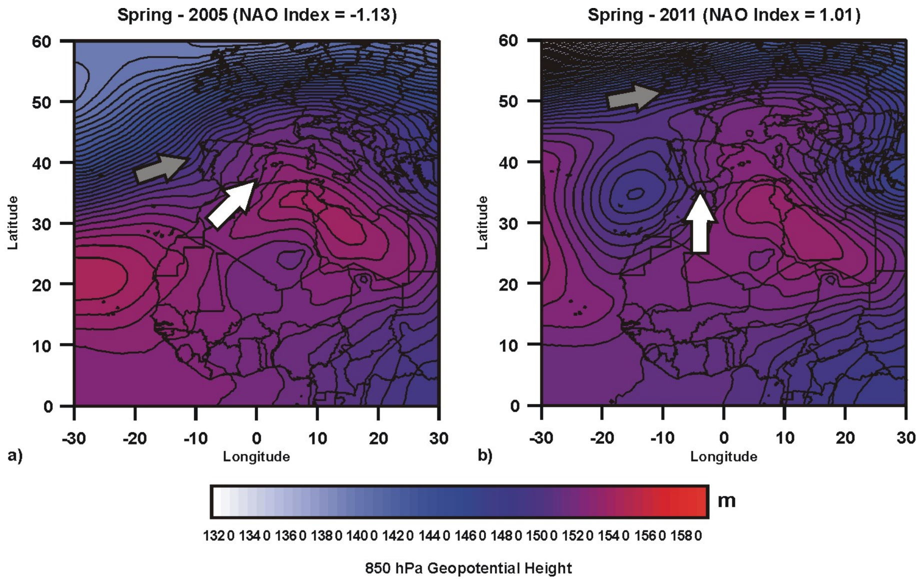


**Fig. 5.** Composite 850 hPa geopotential height (m) during episodic days in spring 2005 **(a)** and 2011 **(b)**. Grey and white arrows indicate Atlantic and African air masses flows, respectively.





ACPD
14, 5495–5533, 2014

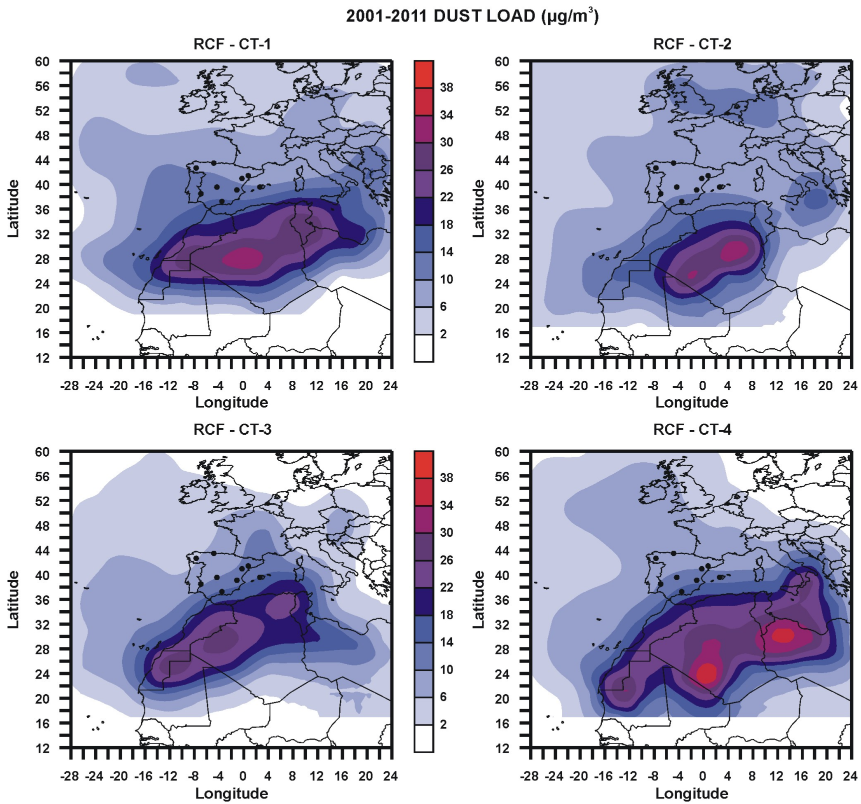


**Fig. 6.** Redistributed concentration fields (RCF) for dust load in $PM_{10}$, during circulation types leading to African Dust Outbreaks (ADO) over the western Mediterranean basin.





ACPD
14, 5495–5533, 2014

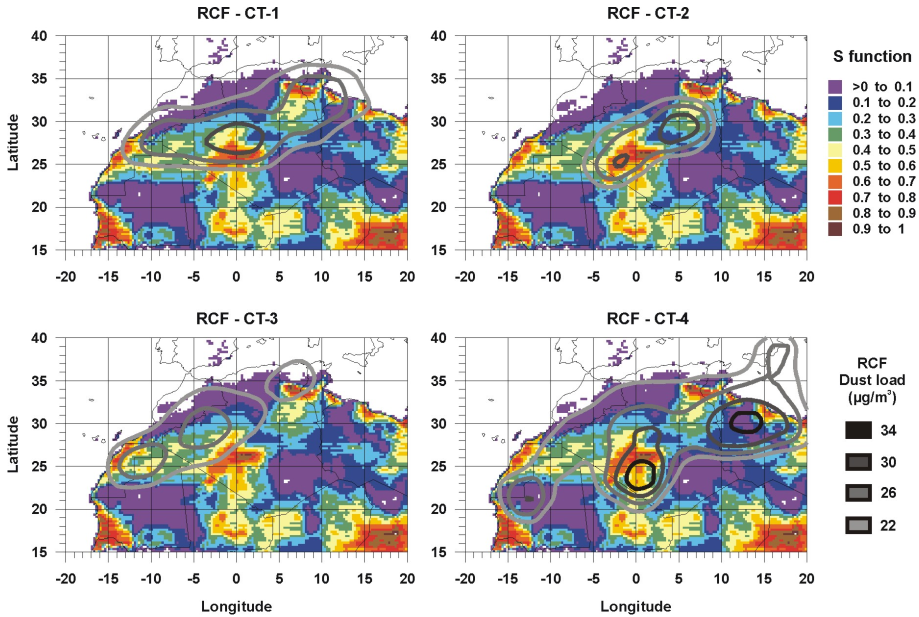


**Fig. 7.** RCF of dust load represented as isolines in the range 22–34 $\mu g\,m^{-3}$ over the geographic distribution of the dust source function *S* (Ginoux et al., 2001). Data obtained from the Atmospheric Physics, Chemistry and Climate Data of the GFDL-NOAA (http://www.gfdl.noaa.gov/atmospheric-physics-and-chemistry_data).





ACPD
14, 5495–5533, 2014

African dust outbreaks over the western Mediterranean basin

P. Salvador et al.

Title Page
Abstract | Introduction
Conclusions | References
Tables | Figures
◀| |▶
◀ ▶
Back | Close
Full Screen / Esc
Printer-friendly Version
Interactive Discussion

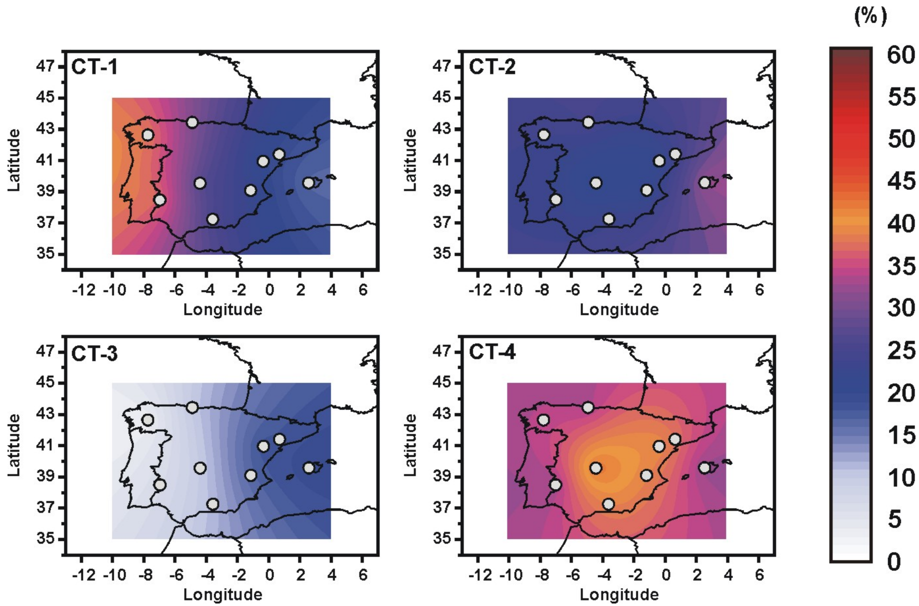


**Fig. 8.** Interpolation maps of the Impact Index (II) estimated at the regional background stations, during circulation types leading to African Dust Outbreaks (ADO) over the western Mediterranean basin in the period 2001–2011.





ACPD
14, 5495–5533, 2014